Fiber Bragg Based Sensors for Foot Plantar Pressure Analysis

Arnaldo G. Leal-Junior[1], M. Fátima Domingues[2], Rui Min[3],
Débora Vilarinho[4], Antreas Theodosiou[5], Cátia Tavares[4],
Nélia Alberto[2], Cátia Leitão[4], Kyriacos Kalli[5],
Anselmo Frizera-Neto[1], Paulo André[6], Paulo Antunes[2,4],
and Carlos Marques[2,4(✉)]

[1] Telecommunications Laboratory, Electrical Engineering Department,
Federal University of Espírito Santo, Fernando Ferrari Avenue, Vitoria,
ES 29075-910, Brazil
[2] Instituto de Telecomunicações, Campus Universitário de Santiago,
3810-193 Aveiro, Portugal
carlos.marques@ua.pt
[3] ITEAM Research Institute, Universitat Politècnica de València,
Valencia, Spain
[4] Department of Physics and I3N, University of Aveiro,
Campus Universitário de Santiago, 3810-193 Aveiro, Portugal
[5] Photonics and Optical Sensors Research Laboratory (PhOSLab),
Cyprus University of Technology, 3036 Limassol, Cyprus
[6] Instituto de Telecomunicações and Department of Electrical and Computer
Engineering, Instituto Superior Técnico, University of Lisbon,
1049-001 Lisbon, Portugal

Abstract. Gait analysis is of major importance in physical rehabilitation scenarios, lower limbs diseases diagnosis and prevention. Foot plantar pressure is a key parameter in the gait analysis and its dynamic monitoring is crucial for an accurate assessment of gait related pathologies and/or rehabilitation status evolution. It is therefore critical to invest effort in research for foot plantar analysis technologies. From that perspective, optical fiber sensors appear to be an excellent solution, given their sensing advantages for medical applications, when compared with their electronic counterparts. This chapter explores the use of optical fiber Bragg grating (FBG) sensors, both in plastic and silica optical fiber, to dynamically monitor the foot plantar pressure. An array of FBGs was integrated in a specially designed cork insole, with the optical sensors placed at key pressure points for analysis. Both insoles, containing plastic and silica optical fiber sensors, were tested for dynamic gait monitoring and body center of mass displacement, showing the reliability of this sensing technology for foot plantar pressure monitoring during gait motion.

Keywords: Fiber Bragg Gratings · Foot plantar pressure · Polymer optical · Fiber · Silica optical fiber · Gait analysis

1   Introduction

Improvements to the quality of life and advances in medicine have resulted in the continuous increase of population lifetimes with enhancements to aging, and this requires the rigorous health monitoring of elderly citizens [1]. Thus, there is a demand for continuous and dynamic health monitoring systems for the assessment and control of the person's physical incapacities [2].

Motion is among the different, key monitoring parameters for human health assessment, and in particular gait analysis is an important indicator of the health condition of a person. As part of the gait analysis method, foot plantar pressure can provide a foot pressure distribution map, where the development or evolution of foot ulcerations, of particular importance for diabetes patients, can be assessed [3]. The foot plantar pressure is an indicator of the gait pattern, which can provide information for the clinicians regarding a gait related pathology [4]. In addition, gait pattern analysis is needed for the application of robotic control devices used for gait assistance [5].

Generally, plantar pressure monitoring is performed with force plates or platforms. Although they can provide accurate measurements of the 3-D dynamics of the foot, they lack portability [6], which is undesirable for dynamic applications, such as in wearable robotics, and they cannot be employed as wearable sensors for remote monitoring. In addition, when a platform is fixed on the ground, the patient may alter their natural gait pattern in order to place the foot within the platform boundaries, which leads to incorrect evaluation of the patient [7]. Although the platform can be hidden in the ground to reduce this effect, several tests need to be performed to obtain a natural gait pattern with the foot within the platform boundaries, which results in a time-consuming process [8].

To mitigate the platform's limitations, instrumented insoles were developed, to be used inside a shoe, thereby resulting in a portable device that could assess the human gait outside the laboratory environment [6]. The advantageous features of instrumented insoles allow the plantar pressure assessment to occur in daily activities, which may lead to a better approximation of the natural gait pattern of the patients or users. However, insoles are generally based on electronic sensors, which, in some cases, lack in stability and resistance to impact loads and so can present measurement errors and inconsistencies [6].

In comparison with electronic sensors, optical fiber sensors (OFSs) present intrinsic advantages related to their compactness, lightweight, multiplexing capabilities, electrical isolation, electromagnetic field immunity and biocompatibility [9]. By exploiting these advantages, OFSs have been applied for the measurement of temperature [10], strain [11], humidity [12], refractive index [13], angle [14], liquid level [15] and pressure [16].

There are two major types of optical fibers: silica optical fibers (SOFs) and polymer optical fibers (POFs). Although SOFs offer lower optical attenuation, POFs have advantages regarding their material features [17]. These features include higher strain limits, higher fracture toughness, flexibility in bending and impact resistance [17]. However, the glass transition temperature of the POFs is only about 100 °C, which leads to a variation of their properties and can limit their applications at temperatures exceed the glass transition temperature [18].

There are many different approaches and mechanisms for optical fiber sensing that may include the measurement of intensity-variation [19], the use of interferometers for phase measurements [20], nonlinear effects [21] and wavelength modulation or change [22]. The latter option uses fiber Bragg gratings (FBGs), which are periodic perturbations of the refractive index of the fiber core along the longitudinal axis of the optical fiber, where a specific wavelength (the Bragg wavelength) is reflected [23]; this is essentially a wavelength selective mirror. Such a grating structure can be obtained by using lasers to modify the optical fiber, and this can take several forms, such as ultraviolet (UV) laser irradiation through a phase mask [23] or direct-write of the grating pattern in the fiber core using a femtosecond (fs) laser [24]. In FBG-based sensors, the shift of the reflected wavelength as a function of the monitored parameter is evaluated. The FBG is intrinsically sensitive to temperature and strain, following Eq. (1) [25]:

$$\Delta\lambda = [(\alpha + \xi)\Delta T + (1 - P_e)\Delta\varepsilon]\lambda_B \qquad (1)$$

where $\Delta\lambda$ is the Bragg wavelength shift, λ_B is the Bragg wavelength, P_e is the photoelastic constant, α is the thermal expansion coefficient of the fiber, ξ is the thermo-optic coefficient, ΔT is the temperature variation and $\Delta\varepsilon$ is the strain variation. Furthermore, the FBG may be embedded in different structures to measure parameters such as force or pressure. For instance, if the FBG is embedded in a diaphragm, the pressure applied to the diaphragm can result in fiber strain following Hooke's law [26].

This chapter discusses the use of a FBG-based sensor network for plantar pressure monitoring, by taking advantage of the special properties provided by OFSs, and in particular FBG-based sensors. The focus of our application considers the increasing demand for monitoring physical parameters for elderly citizens and populations in general. The sensor network is compact and portable and this was achieved by embedding the sensors in a cork insole. In order to address the advantages offered by both SOFs and POFs and to compare their performance, the instrumented insole was developed first with FBGs inscribed in SOFs, followed by a similar system developed with POFs.

After this initial introduction, Sect. 2 presents an overview of foot biomechanics including its structure, movements and plantar pressure distribution during the gait motion. This section also comprises/contains the system requirements, the insole production and tests protocols. In Sect. 3, the insole development with SOFs is discussed, whereas in Sect. 4, the FBG-based insole with POFs is proposed. Finally, the main conclusions are presented in Sect. 5.

2 System Requirements and Insole Production

2.1 Foot Plantar Pressure Overview

The human foot provides the support and balance when a person is in a standing position and acts to ensure body stabilization during the gait motion [27]. In order to provide such crucial role in daily activities and locomotion, the foot is a multi-articular

structure comprising soft tissues, bones and joints. In total, the human foot has 26 bones, which are divided as 7 tarsals, 5 metatarsals and 14 phalanges. Regarding the joints, there are the ankle, subtalar, midtarsal, tarsometatarsal, metatarsophalangeal and interphalangeal [27]. Such a complex structure is divided in to four main segments: hindfoot, midfoot, forefoot and phalanges, which are presented in Fig. 1.
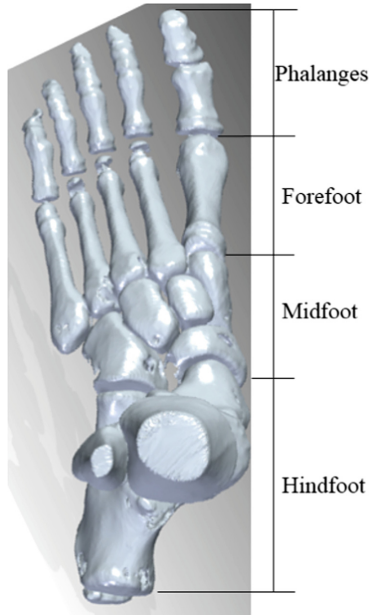

Fig. 1. Top view of the left foot structure divided in to the four main segments.

Extrinsic and intrinsic muscles are responsible for the control of the joints presented in Fig. 1, which provide support for the foot and its motion [6]. The human motion generally occurs in 3 planes of motion, which are defined as sagittal, frontal and transverse planes [28]. The foot movements that occur in the sagittal plane are the plantarflexion and dorsiflexion (Fig. 2(a)), whereas in the transversal plane, there is the foot abduction and adduction (Fig. 2(b)). In addition, the movements in the frontal plane are the foot inversion and eversion (Fig. 2(c)). There is also a combination of these movements (pronation and supination). The foot is pronated when there is simultaneous abduction, eversion and dorsiflexion. On the other hand, the foot is supinated when the opposite occurs, i.e., it is simultaneously adducted, inverted and plantar flexed [27].

Conventionally, the gait cycle is delimited from the initial contact with one foot until the same foot touches the ground again, and this is divided in stance and swing phases [28]. The percentage of each phase varies with the gait velocity, but generally the stance phase represents 62% of the cycle [29]. Both stance and swing phases have
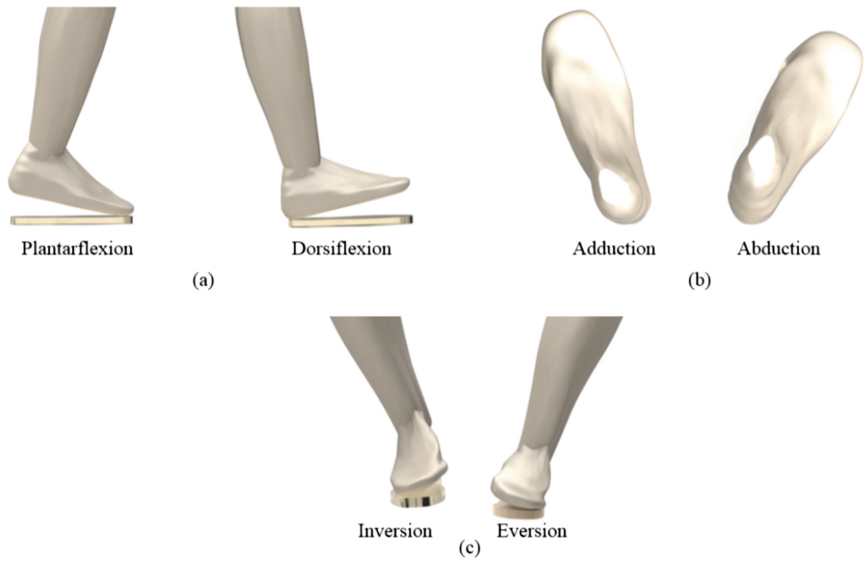
Fig. 2. Representation of different movements for the foot: (a) plantarflexion and dorsiflexion, (b) adduction and abduction and (c) inversion and eversion.
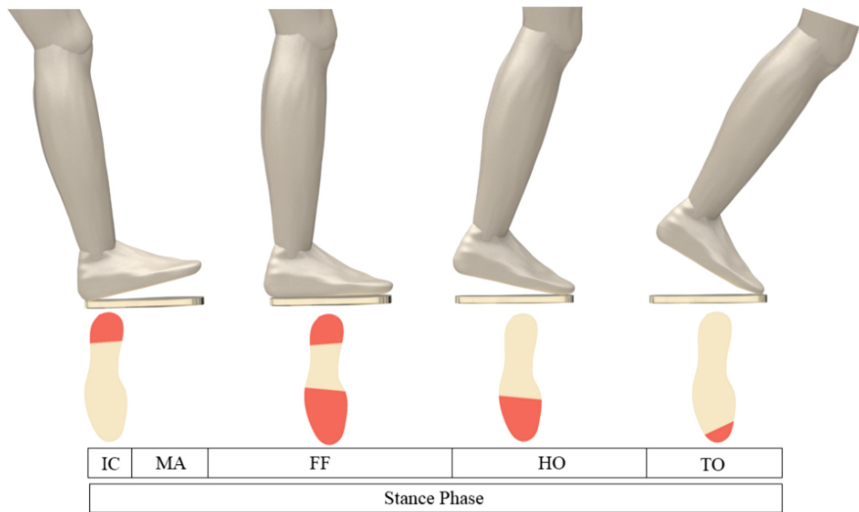
Fig. 3. Plantar pressure distribution during the stance phase of the gait cycle. The length of each subdivision is presented for illustration proposes only and the actual length of each phase varies with the person's gait.

subdivisions [6], nevertheless we will only present those of the stance phase, since this is the one detected by the proposed insole. Regarding the adopted stance phase subdivisions, it begins with the initial contact (IC), which is the first contact of the foot

with the ground. Then, there is the maximum weight acceptance (MA) when the heel is in full contact with the ground and the entire person's weight applied. Following this phase, there is the foot flat (FF), which is characterized by the rotation of the foot until it is in complete contact with the ground. In this gait event, a stable support of the body is achieved. Thereafter, the body starts to roll over the foot with the ankle as a pivot and the center of mass is also moved forward. In this event, the heel loses contact with the ground, at the heel off (HO) phase. The final subdivision of the stance phase is the toe off (TO), when the toe loses contact with the ground and, then, the swing phase starts [6]. Figure 3 presents the aforementioned stance phase subdivisions and the plantar pressure involved at each subdivision. We note that the length of each subdivision varies with the gait parameters and the subdivision presented is only for illustration proposes.

2.2   Insole Development

As discussed in the previous sections, the gait parameters and plantar pressure assessment is a complex measurement. Therefore, the design of the device able to monitor such values should comply with the requirements listed below [6]:

- Lightweight: the insole weight is important for the user mobility and should not change his/her natural gait pattern.
- Limited cabling: this feature guaranties a comfortable and safe system, where excessive use of cables can make the system less safe due to the possibility of accidents if the person tangles with the cables.
- Shoe and sensor placement: the sensors need to be located in the regions with higher plantar pressure and distributed to acquire the dynamic measurements of the plantar pressure in the whole foot.
- Linearity: a linear response generally leads to higher simplicity in the signal processing and lower errors for the sensors.
- Temperature sensitivity: the sensors need to have low temperature sensitivity or present temperature compensation in a range of temperatures typically from 26–37 °C [6].
- Pressure range: The pressure range is the key specification, since it defines the range of patients that can use the technology. Foot plantar pressure can reach values as high as 1900 kPa, as typically reported in the literature, thus the sensor must be able to withstand this level of pressure [6].
- Sensing area of the sensor: the sensors need to be small to accurately measure the plantar pressure, since sensors with large sensing areas may underestimate the plantar pressure due to the force distribution in a large area, which results in lower measured pressure.
- Operating frequency: since the gait is a dynamic event, a precise plantar pressure assessment involves sampling frequencies as high as 200 Hz [6].

In order to achieve the requirement regarding the sensor positioning, 5 sensing points were chosen, following the regions known to have higher plantar pressure, as defined in [30]. The 5 sensing regions were chosen to coincide with the key regions in a distributed manner, as shown in Fig. 4.
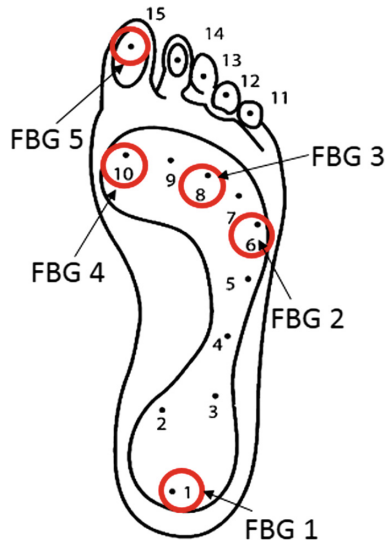
**Fig. 4.** Plantar pressure region and the chosen measurement points.
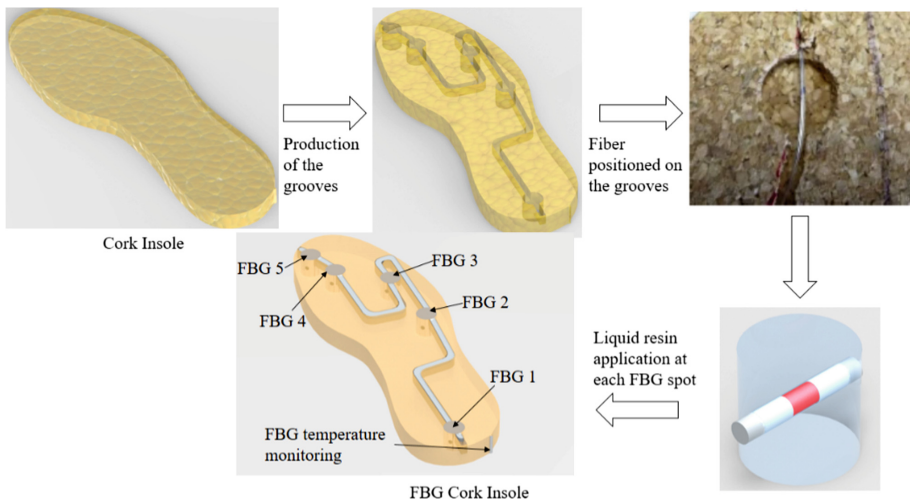
Fig. 5. Instrumented cork insole production steps.

The 5 FBGs sensors, distributed according to Fig. 4, were embedded in a cork insole with 10-mm thickness. The fabrication methodology for both SOF and POF-based FBG-embedded insoles was similar, with the type of fiber used representing the main difference between the insoles [1, 31]. The first step for the instrumented insole fabrication was to machine a cork plate to give it an insole shape. Then, a groove with 2.5-mm depth and 2.0-mm width was carved in to the cork sole, paving the way to place the optical fiber. In the key points of analysis, a cylinder of 10-mm diameter was

also carved, as shown in Fig. 5. The cork material was chosen to produce the insoles due to desirable properties, including the cork thermal isolation, malleability and low Poison ratio that prevents the crosstalk between the sensors [1, 32]. In each carved cylinder, an epoxy resin (Liquid Lens^{TM}, Bedford, Bedfordshire, UK) was applied to encapsulate the FBGs. Thus, each sensor was composed of a cylindrical epoxy resin structure with the FBG located in the middle. The strain, applied in the resin when the cylinder was pressed, was directly transmitted to the FBG, leading to a Bragg wavelength shift. In addition to the strain variations, the FBGs were also sensitive to temperature changes (see Eq. (1)) and, for this reason, an additional FBG was positioned on the side of the insole (see Fig. 5) and, therefore, isolated from the plantar pressure. This isolated FBG monitored and compensated any temperature effects in the sensors' response. Nevertheless, the cork insole provided thermal isolation to the sensors and the temperature effects were already significantly reduced [1]. Figure 5 summarizes the instrumented insole production.

The FBG-embedded insole was connected to a portable interrogation system composed of a battery, a miniaturized broadband optical ASE module (B&A Technology Co., As4500), an optical circulator (Thorlabs, 6015-3), and an optical spectrometer (Ibsen, I-MON 512E-USB). The optical spectrometer operated with a maximum acquisition rate of 960 Hz and a wavelength resolution of 5 pm. This equipment was used for the acquisition of the reflected Bragg wavelength as a function of time during the plantar pressure monitoring tests (see Fig. 6).


Ibsen I-MON E
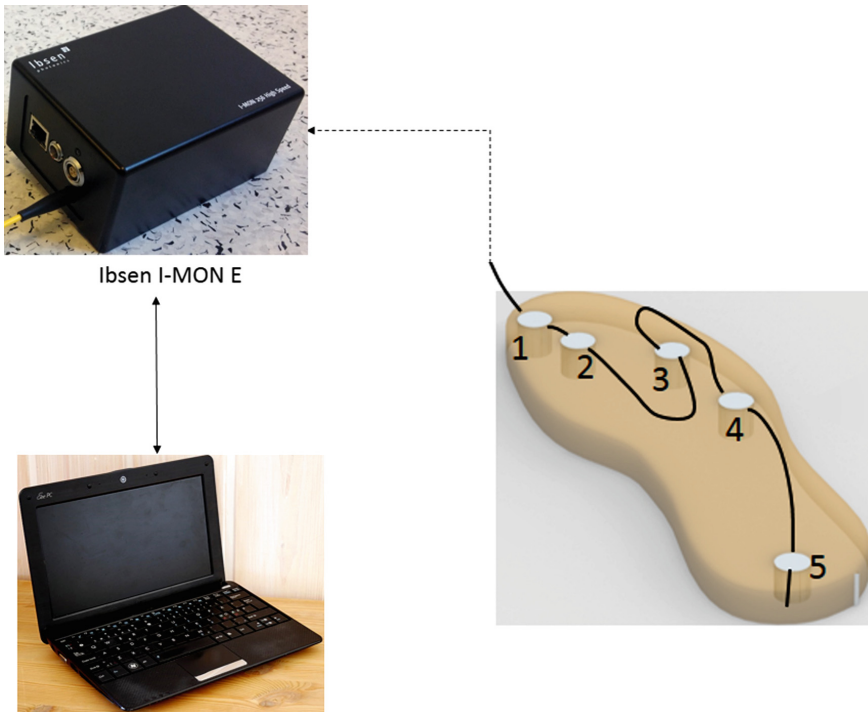
Fig. 6. Schematic representation of the instrumented insole monitoring system.

2.3   Experimental Protocols

In the first test, the FBG array with sensing elements were calibrated in a universal mechanical testing machine (Shimadzu® AGS-5Knd, Columbia, SC, USA) from 0 to 1500 kPa, as shown in Fig. 7. The loads were applied independently at each sensing point, FBG 1 to FBG 5, using a probe with a diameter of 10 mm (the same diameter as the epoxy resin cylinder). The response of each sensor with respect to predefined pressures was acquired, it was possible to evaluate each sensors' sensitivity and linearity. In addition, the characterization tests were made at a constant temperature of 22 °C to reduce the effect of this parameter in the sensors' response.
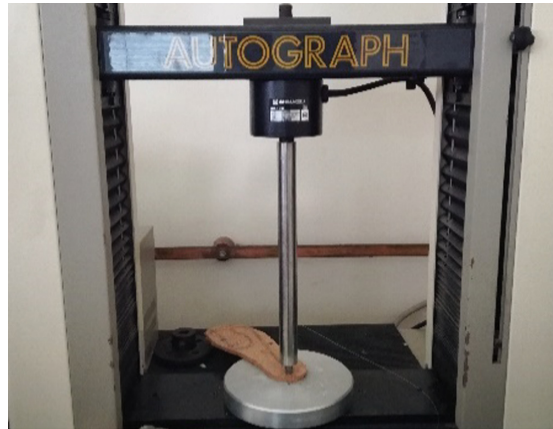

Fig. 7. Experimental setup for the FBG-based instrumented insole pressure characterization.

Fig. 8. Experimental setup for the proof-of-concept test with the instrumented insole acting as a fixed platform (adapted from [1]).

The second proposed test was the evaluation of plantar pressure during a normal gait, but with the insole fixed to the ground (as a force platform). This test was made as a proof-of-concept for the proposed FBG-embedded sensor system. The response of each sensing point, as well as the sum of all sensors were analyzed, and the tests were repeated 5 times. Figure 8 shows a schematic representation of this test protocol.

In the third test, the body center of mass (BCM) displacements for different movement planes was evaluated. The movements are in the frontal plane, following the movement of the subject's torso to left and right and on the sagittal plane, where the volunteer was requested to move the body forward and backward. The subject was asked to stand on the sensing platform, with one foot on the sensing area and the other leveled in the same horizontal plane, to execute a series of B M movements (of ∼3-s duration each). The protocol is summarized in Fig. 9. The test started with the subject standing still at the center position (C). This was followed by the BCM movement forward in the sagittal plane to achieve the anterior (A) position, and followed by the movement back to the center (C). The last movement in the sagittal plane was to the posterior (P) position and, once again, arriving at the center (C). The displacement in the frontal plane was executed with an analogous procedure. In this case, the BCM was moved to the left (L) and right (R), always followed by the return to the center position.
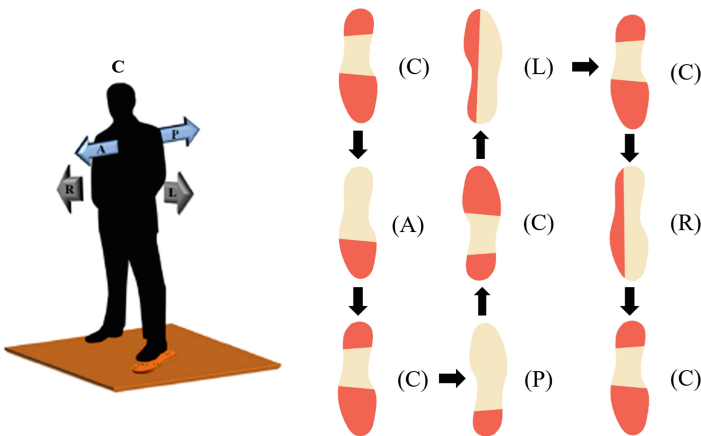
Fig. 9. Schematic diagram of the protocol implemented for the analysis of the BCM displacement to the right, whereas the positions and plantar pressure points are presented to the left (adapted from [1]).

Finally, the proposed insole was adapted to a shoe for pressure monitoring during the gait cycle (Fig. 10), as a portable solution for the plantar pressure assessment. The subject, whilst wearing the shoe with the instrumented insole, was asked to walk in a straight path with predefined distance, while the gait cycles were analyzed.

Fig. 10. FBG-embedded insole positioned inside a shoe for plantar pressure monitoring during the gait motion.

3 SOF-FBG-Based Instrumented Insole

The first approach analyzed was the FBG-embedded insole with the Bragg gratings inscribed in SOF, in this case GF1-photosensitive optical fiber (Thorlabs), using the "phase mask technique". The laser employed was an UV pulsed KrF excimer laser (Bragg Star Industrial-LN), operating at 248 nm, applying pulses with energy of 5 mJ and repetition rate of 500 Hz. The gratings had a physical length of 1.5 mm. The phase masks that were used were customized for 248-nm UV lasers in order to produce FBGs in the 1550-nm spectral region (Ibsen Photonics). Figure 11 shows the reflection spectrum of an FBG array with the 5 sensing elements, inscribed in the SOF with the aforementioned setup.
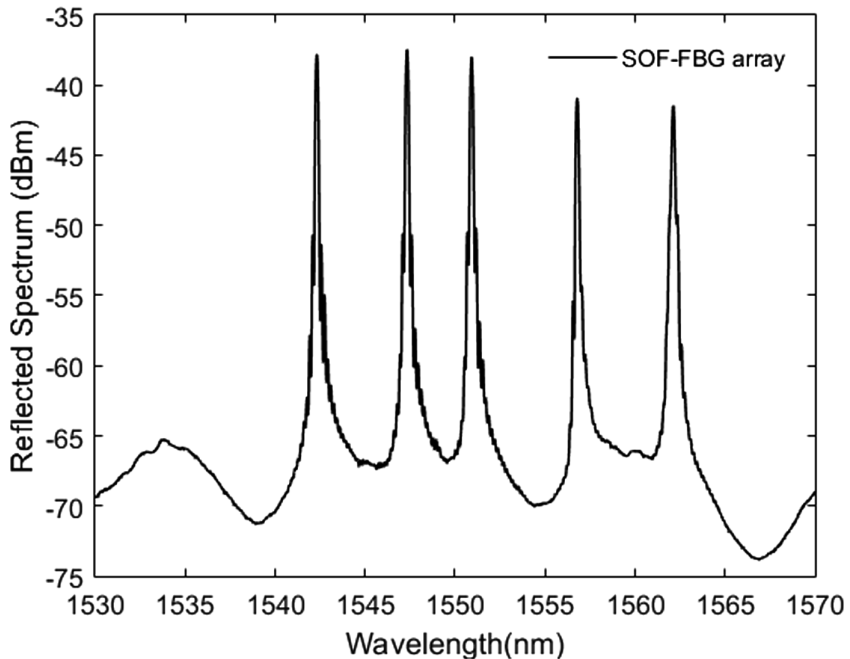
**Fig. 11.** Reflection spectrum of the FBG array inscribed in the SOF.

Figure 12 shows the calibration results for each FBG in the SOF-based system. The sensors display a linear response in all cases. However, the sensitivity shows a higher variation between each sensor point. Besides the differences in the reflected Bragg wavelength, this discrepancy could be related with the incorporation process in the insole. Since the cork is a porous material, different amounts of the epoxy resin may have infiltrated into its surroundings, which leads to different positions of the FBGs in the epoxy resin cylinders [1]. Thus, different pressure-induced strains are transmitted to the FBG. In this case, the lowest sensitivity was found for the FBG 4 (0.27 pm/kPa), whereas FBG 2 presented the highest sensitivity (0.87 pm/kPa). The linearity of each sensor was also analyzed considering its determination coefficient (R^2), shown in Fig. 12. In this case, all the sensors showed a linearity greater than 0.990, except the FBG 4. The low linearity (0.956) could be related with the incorporation process of the grating in to the cork insole, as discussed above.
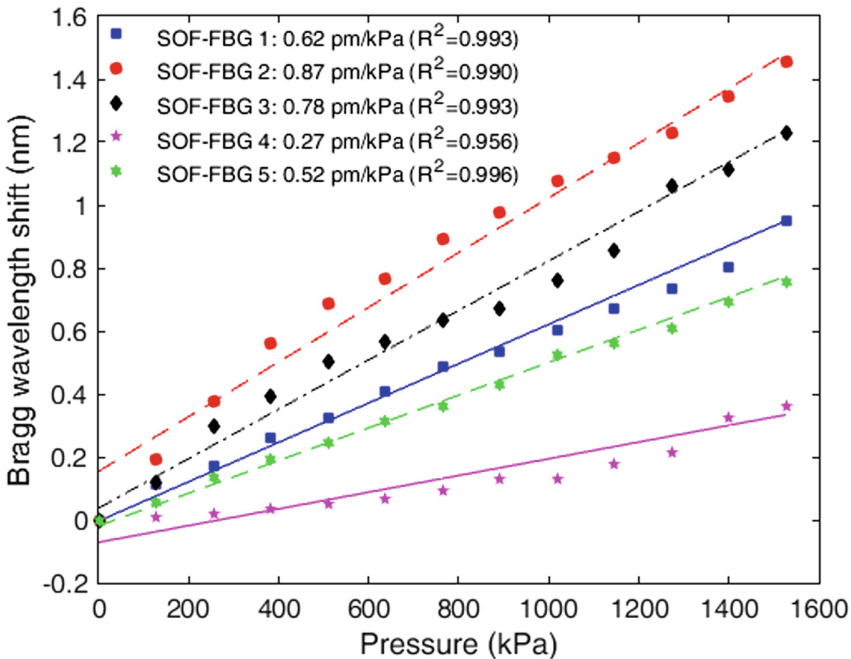
Fig. 12. Bragg wavelength shift as a function of the applied pressure in the SOF-FBGs characterization tests (adapted from [1]).

In the second test, where the FBG-embedded insole is fixed to the ground, it is possible to obtain the sequence in which the sensors are activated and the plantar pressure associated with each point under analysis. The maximum pressure was registered by each sensor according to the expected gait event sequence detailed in the previous section [1].

The stance period is initiated when the heel touches the ground, IC; after the contact of the heel with the ground, there is the first peak in the sensors responses (MA phase); in these events, FBG 1 presents the highest pressure. The foot is then moved toward a stable support position for the body in which the hip joint becomes aligned with the ankle joint (FF phase), where all five FBGs are under pressure. Thereafter, the heel loses contact with the ground in the HO phase, which results in a drop in the pressure measured by FBG 1, the pressure in the FBG 2 is also reduced, whereas the FBGs 3, 4 and 5 show an increase in the measured pressure. Finally, there is the TO phase, where all FBGs presents null pressure, which indicates that the foot is not in contact with the ground and the swing phase is about to start. Figure 13 shows the response of each FBG during a complete phase stance. In addition, the gait events detected are shown with respect to the stance phase percentage.
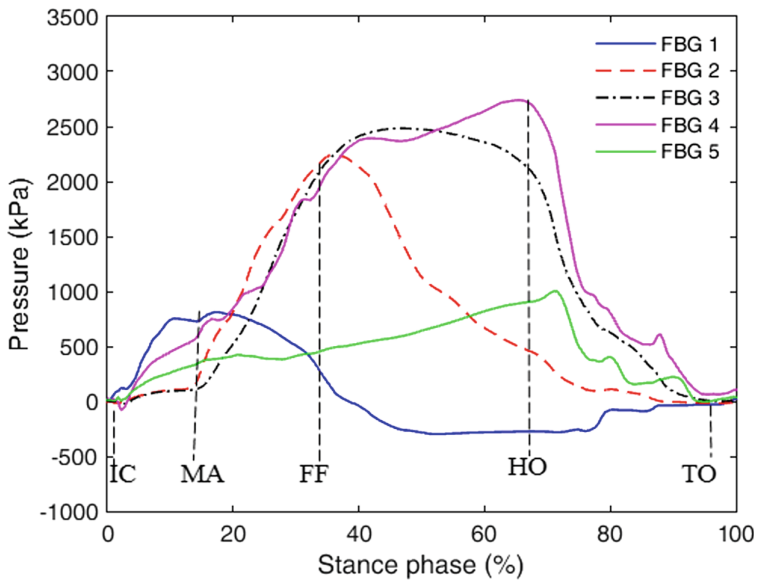
Fig. 13. Plantar pressure during the stance phase in the force platform application (adapted from [1]).

Regarding the BCM displacement tests, the Bragg wavelength shift of each sensor is presented as a function of time in Fig. 14. In the first pose (C), corresponding to the subject without BCM displacement, all the sensors are activated. Then, in the anterior movement (A), there is an increase of the pressure in the sensors positioned in the metatarsal and toe areas (FBGs 4 and 5), while the sensor placed in the heel section indicates a decrease of the plantar pressure when compared with the position (C). Similarly, during the BCM posterior displacement (P), the opposite occurs, with increase of the pressure in FBG 1 and 2. Regarding the frontal plane displacements, when the BCM is dislocated to the right, there is an increase of the pressure in FBG 2, whereas FBG 4 experiences an increase in the pressure when the BCM is moved to the right.
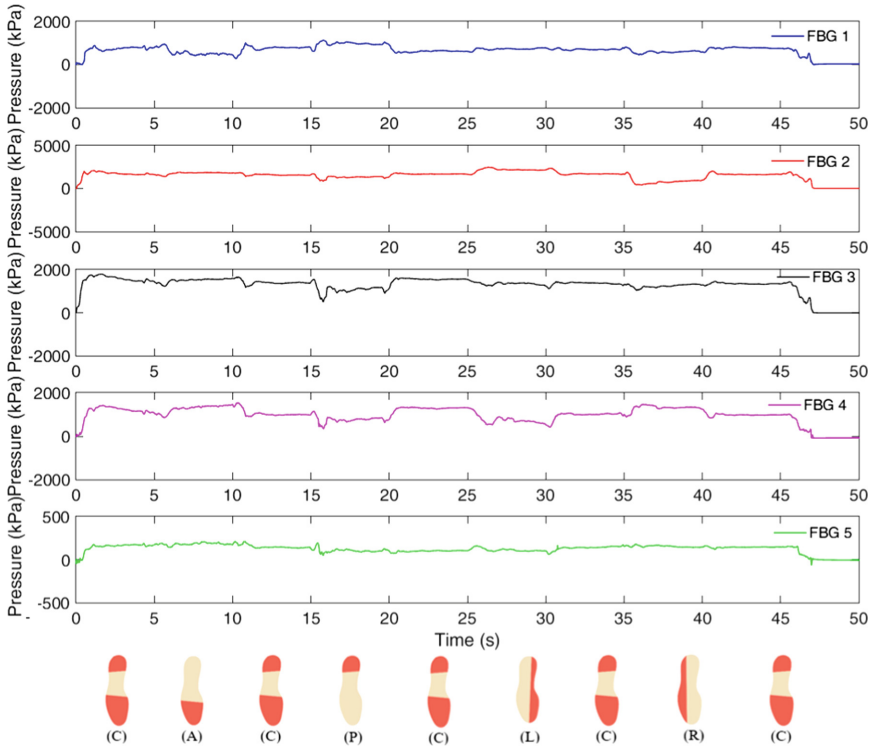
Fig. 14. SOF-FBG results in the BCM displacement test (adapted from [1]).

Regarding the last set of tests, namely gait cycle analysis, the subject, a 45-kg female, was instructed to walk with a velocity that she found to be comfortable. Meanwhile, the Bragg wavelength was acquired by the interrogation system. Figure 15 presents the plantar pressure obtained in three consecutive gait cycles, where similar behavior was recorded when compared with the fixed platform test. The element that was initially actuated was in the heel area (FBG 1), followed by the metatarsal area (FBG 2, 3 and 4) and, finally, the element in the toe (FBG 5), at the conclusion of the stance phase. Moreover, the different phases in the gait cycle can be identified, namely the stance phase (this characterizes ∼68% of the cycle) and the swing phase. The duration of the stance phase can be related to the subject gait velocity and spatial parameters [29]. The swing phase is characterized by the absence of measured pressure by the instrumented insole.
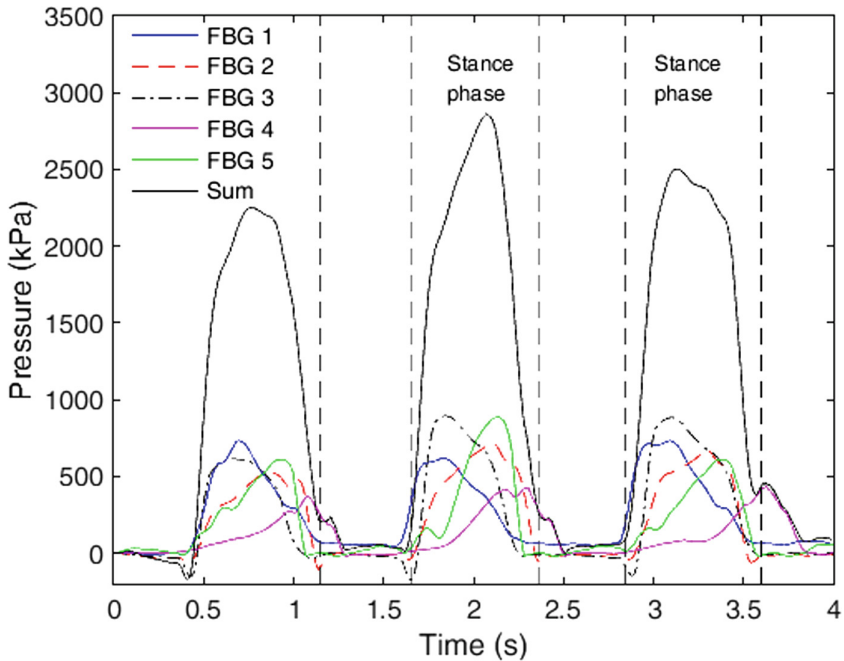
Fig. 15. SOF-FBG results in the in-shoe gait monitoring application (adapted from [1]).

4   POF-FBG-Based Instrumented Insole

After the initial development of a FBG-embedded insole using SOFs, the next version of the instrumented insole was based on POFs. The advantages of using POFs in the plantar pressure assessment are related to the material having a lower Young's modulus that leads to a higher sensitivity compared with the similar SOF sensors. In addition, POFs can withstand strain of approximately 10%, whereas SOF typically have strain limits of ∼1% [17]. Thus, in a rough estimation, the insole based on POFs can support a pressure 10 times greater than the SOF-based device, assuming that both sensors are incorporated into the insole under the same conditions. These latter advantages mean that the POF-based insole can be used with patients having greater body mass.

The FBG sensors employed in the experiments were inscribed in a gradient index multimode CYTOP fiber (Chromis Fiberoptics Inc., Warren, NJ, USA) with core diameter of 120 μm, a 20 μm cladding layer, and an additional polyester and poly-carbonate over-cladding structure to protect the fiber, resulting in a total diameter of 490 μm [33]. For the POF-FBG inscription, the plane-by-plane femtosecond laser inscription method was used [24]. Regarding the setup for the gratings inscription, a fs laser system (HighQ laser femtoREGEN) operating at 517 nm with 220 fs pulses duration was used to modify the material [24]. All the inscriptions were performed without removing the outer protection jacket, and the fiber samples were immersed in matching oil between two thin glass slides. In addition, the samples were mounted on

an air-bearing translation stage system (Aerotech) for accurate and controlled 2D motion (nanometer precision) during the inscription process. The laser beam was focused from above through an x50 objective lens (Mitutoyo). By accurately controlling the focused beam, refractive index modifications can be induced in the center of the fiber's core without influencing the intermediate layers. The pulse energy was ∼80 nJ, whereas the repetition rate was controlled using a pulse picker and set at 5 kHz. The physical length of the gratings was ∼1.2 mm and the grating size was controlled, having a plane width across the center of the core of 15 μm in order to minimize the coupling between the higher order modes of the fiber and the grating. Figure 16 illustrates the reflection spectrum of the POF-FBG array inscribed with the methodology mentioned above.
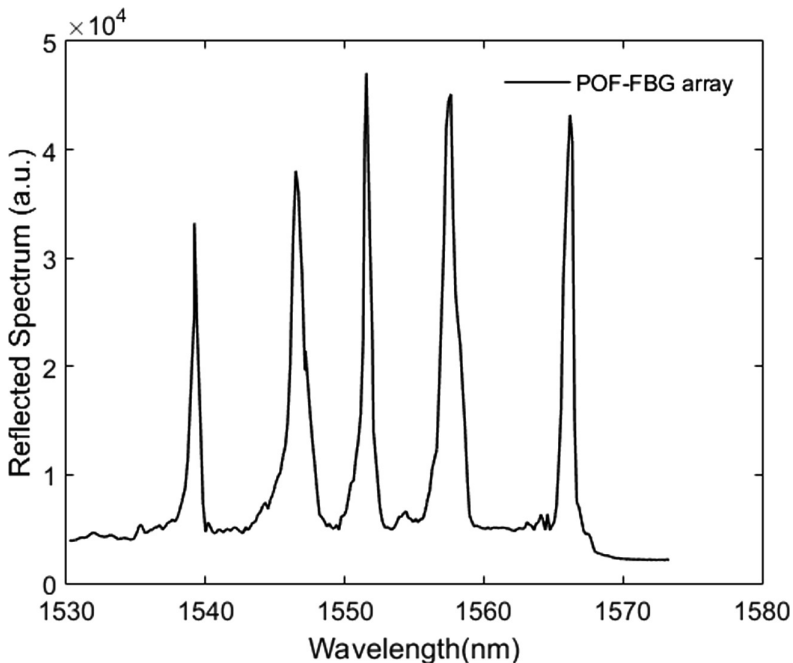
Fig. 16. Reflection spectrum of the FBG array inscribed in the POF.

Following the grating inscription, the FBGs were incorporated in the cork insole as presented in Sect. 2, and the tests were made with the protocols already discussed in the same section and also applied to the SOF-based insole. Therefore, the first test was the calibration of each POF-FBG in the universal mechanical testing machine. The calibration for all sensing elements are depicted in Fig. 17, where a linear dependence of the Bragg wavelength shift with the applied pressure is obtained (mean R^2 higher than 0.990).
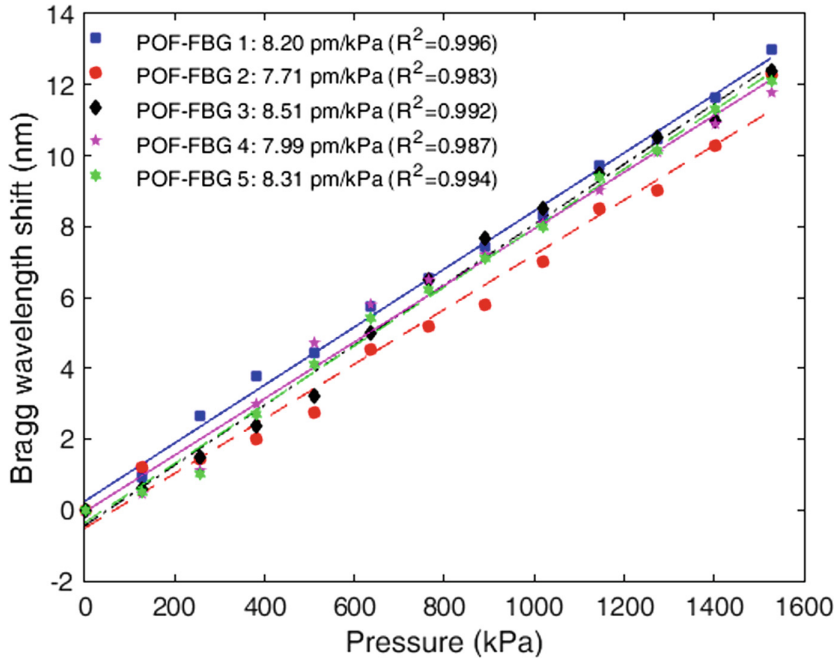
Fig. 17. Bragg wavelength shift as a function of the applied pressure in the POF-FBGs characterization tests.

In order to have a broader comparison with the SOF-based sensor system, Table 1 summarizes the sensitivity coefficients for all POF and SOF sensors. By comparing the values obtained for the SOF-based insole, the POF-FBG insole shows higher sensitivity for all the 5 FBGs, as anticipated based on the material advantages. The lowest sensitivity obtained for the POF-FBGs is 7.71 pm/kPa, whereas, for the silica FBGs is 0.27 pm/kPa. Regarding the mean value of pressure sensitivity, the values obtained are 8.14 pm/kPa and 0.61 pm/kPa, for the POF-FBGs and SOF-FBGs, respectively. The Young's modulus of the CYTOP is ~ 4 GPa and the silica is ~ 70 GPa [34]. Thus, this

Table 1. Pressure sensitivities obtained at the sensor characterization.

FBG	Pressure sensitivity (pm/kPa)	
	POF	SOF
1	8.31	0.62
2	7.99	0.87
3	8.51	0.78
4	7.71	0.27
5	8.20	0.52

difference corresponds to a factor of about 11, whereas the mean difference between the sensitivities of POF and SOF-based FBGs is a factor of 13. This discrepancy, which is greater in terms of pressure sensitivity in relation to the Young's modulus, should also be related to the incorporation process of the Bragg gratings into the epoxy resin cylinder. The POF-FBGs appear to have been better positioned, thus they also show lower variation in their sensitivity.

The cork insole was subsequently fixed to the ground, and the pressure induced in the sensing elements during a normal gait movement was analyzed, as showed in Fig. 18. The mean response of each sensor is presented for the fixed platform case.
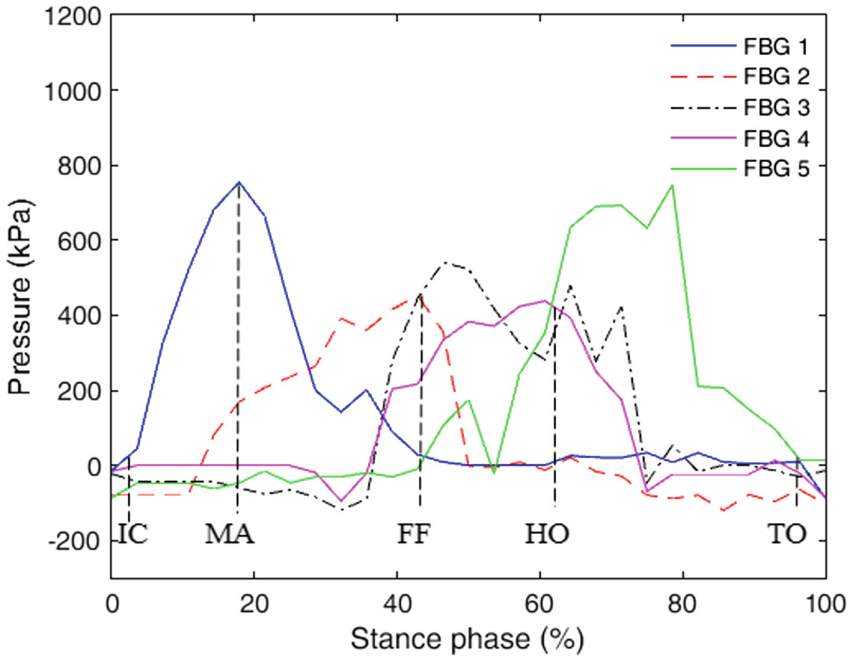
Fig. 18. POF-FBGs response of the tests using the FBG-embedded insole as a fixed force platform.

In Fig. 18, it is possible to observe the activation time for each sensor and its relation to the stance phase of the gait cycle. The FBG 1, located at the heel region, shows a pressure increasing at the beginning of the cycle (IC phase). In addition, FBG 1 exhibits a peak in the MA phase, where there is also an increase of the pressure exerted in the FBG 2, while the other sensors (FBG 3, 4 and 5) do not show a significant variation in the pressure. As the stance phase continues, the responses of FBGs 2, 3 and 4 show a pressure increase, whereas the FBGs 1 and 5 localized in heel and toe regions, respectively, show lower pressure responses than the sensors in the midfoot and forefoot regions. Such behavior is related to the FF phase and, as the cycle continues, there is a decrease in the pressure of the FBGs 1 and 2 until it reaches a null

value in the HO phase. Finally, there is a peak in the FBG 5 (localized in the toe region) and, when its pressure response starts to drop, there is the TO phase, which also indicates the beginning of the swing phase, where all FBGs present negligible pressure values.

The third static test is the assessment of the BCM displacements both in the body sagittal plane, by moving it forward and backwards, and in the frontal plane, with the subject moving the torso from the left to the right and vice-verse. The results for this protocol are presented in Fig. 19.
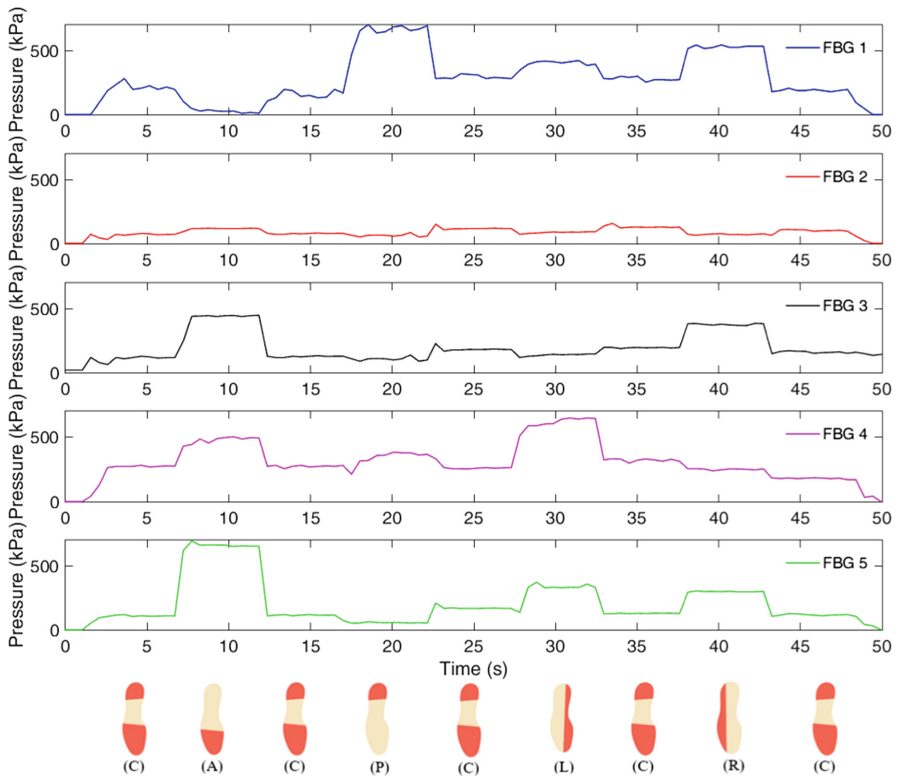

Fig. 19. POF-FBG responses for the BCM displacement tests.

In the center position (C), there is a pressure increase in all POF-FBGs. Regarding the tests on the sagittal plane, the sensors positioned in the metatarsal and toe areas show higher pressure in the anterior movement (A), when compared to the sensors in the heel and midfoot sections. On the other hand, during the posterior displacement of the BCM (P), the pressure increases on FBG 1, positioned at the heel area, whereas the pressure values at the toe and metatarsal areas decrease. However, due to the high sensor sensitivity and fiber positioning in the insole, it is not possible to activate only the heel and toe regions. Thus, the sensors on the metatarsal and midfoot regions are

also activated. This is more evident on the anterior movement, since the subject presents more difficulty to maintain her balance during the test. In the displacements within the frontal plane (left and right displacements), the sensor placed in position 2 records the increase of pressure, when the BCM is displaced to the left (L). Analogously, FBGs 3 and 4 show a pressure increase when the BCM is moved to the right (R). Since the BCM displacement is a combined movement, where the whole foot is involved, there is also the activation of FBGs 1 and 5, positioned on the heel and toe, respectively. In summary, the results obtained on both sagittal and frontal planes show that the proposed sensor system is able to track the BCM displacement with similar results when compared to the literature and the SOF system [35]. In addition, compared to the SOF-FBG results presented in Fig. 14, the POF-FBG response show greater clarity, and are readily interpreted due to their higher sensitivity.

The last set of tests is with the FBG-embedded insole positioned inside a shoe for the gait analysis. Figure 20 shows the responses of each sensor and their sum for three consecutive gait cycles. From the results obtained with the proposed insole sensor network, the repeatability of the data becomes clear, since it presents similar response in all analyzed gait cycles. It is also possible to detect the sequence in which the sensors are activated (maximum amplitude registered), which is in agreement with what is expected for a gait movement [27, 28] and with the SOF-based insole previously presented [1].
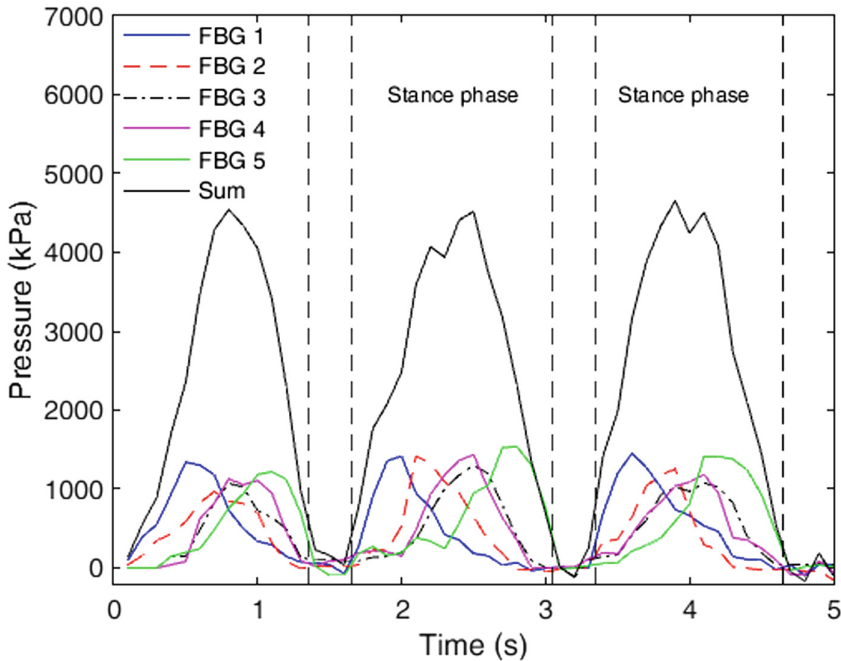
Fig. 20. POF-based instrumented insole response for the plantar pressure assessment during the gait.

At the beginning of the stance phase of the gait cycle, the heel starts its contact with the floor and FBG 1 is activated. The other FBGs respond in sequence with the evolution of the cycle, i.e., first the FBG 1 shows a pressure increase and, as the cycle continues, FBGs 2, 3, 4 and 5 are activated. When all the sensors record negligible pressure, we know that this coincides with the start of the swing phase of the gait cycle. The sum of all sensors is also presented, where we observe the combined effect of the plantar pressure response. In addition, it is possible to infer that the sensors present high repeatability, which is actually limited by the human's ability to repeat the motion, since different gait cycles may not be identical, even for the same person [28]. The dynamic measurements show the capability of the proposed system to detect the subdivisions of the stance phase, discussed in Sect. 2. Such features of the proposed sensor system not only can aid in the detection of gait related pathologies, but also can be applied on the controllers of wearable robots for gait assistance and in eHealth architectures [5, 36].

In general, the results obtained in the POF-based instrumented sole show that in addition to the advantages related to the material features, the employed POF is easier to handle and to incorporate in the cork insole when compared with the SOF system.

To conclude, it is worth to mention that we adopted a 5 FBGs sensors solution embedded in a cork insole with 10-mm thickness and such a thickness can slightly influence and change the walking efforts/capabilities of the walkers. However, from the results of this work, it maintains the same pattern of reaction force found in other systems, for example. Also, 10-mm thickness of the insole is only slightly larger than the conventional insoles. So, if there is influence, we can assume that it is relatively negligible in the context of the work presented here and, the results support this, since we find the same pattern in the ground reaction force curves.

5   Conclusions

The fast technological evolution we have been witnessing in the past decades offers several benefits to healthcare systems and diagnosis methodologies. The presented sensing platforms are reliable and accurate technologies for gait disorder diagnoses and physical rehabilitation evolution analysis. The discussed solutions show a level of performance that meets the electronics devices currently available in the market, with the additional OFS inherent advantages.

Furthermore, the OFS insoles can act as eHealth enablers, in an architecture comprising of a small interrogator system (adapted to a belt), a wireless transceiver and a cloud-based monitoring application [36]. Such architectures can be used to register, in real time, the plantar pressure of users, thereby emitting alerts in case of abnormal values, or even automatically requesting for emergency services in the extreme events, such as the case of a fall. This technology is a very promising eHealth tool.

References

1. Domingues, M.F., et al.: Insole optical fiber Bragg grating sensors network for dynamic vertical force monitoring. J. Biomed. Opt. **22**(9), 91507 (2017)
2. Korhonen, I., Pärkkä, J., Van Gils, M.: Health monitoring in the home of the future. IEEE Eng. Med. Biol. Mag. **22**(3), 66–73 (2003)
3. Morag, E., Cavanagh, P.R.: Structural and functional predictors of regional peak pressures under the foot during walking. J. Biomech. **32**, 359–370 (1999)
4. Leal-Junior, A.G., Frizera, A., Avellar, L.M., Marques, C., Pontes, M.J.: Polymer optical fiber for in-shoe monitoring of ground reaction forces during the gait. IEEE Sens. J. **18**(6), 2362–2368 (2018)
5. Villa-Parra, A., Delisle-Rodriguez, D., Souza Lima, J., Frizera-Neto, A., Bastos, T.: Knee impedance modulation to control an active orthosis using insole sensors. Sensors **17**(12), 2751 (2017)
6. Hadi, A., Razak, A., Zayegh, A., Begg, R.K., Wahab, Y.: Foot plantar pressure measurement system: a review. Sensors **12**, 9884–9912 (2012)
7. Sanderson, D.J., Franks, I.M., Elliott, D.: The effects of targeting on the ground reaction forces during level walking. Hum. Mov. Sci. **12**(3), 327–337 (1993)
8. Ballaz, L., Raison, M., Detrembleur, C.: Decomposition of the vertical ground reaction forces during gait on a single force plate. J. Musculoskelet. Neuronal Interact. **13**(2), 236–243 (2013)
9. Webb, D.J.: Fibre Bragg grating sensors in polymer optical fibres. Meas. Sci. Technol. **26**(9), 92004 (2015)
10. Zhu, T., Ke, T., Rao, Y., Chiang, K.S.: Fabry-Perot optical fiber tip sensor for high temperature measurement. Opt. Commun. **283**(19), 3683–3685 (2010)
11. Minakawa, K., Mizuno, Y., Nakamura, K.: Cross effect of strain and temperature on Brillouin frequency shift in polymer optical fibers. J. Light. Technol. **35**(12), 2481–2486 (2017)
12. Rajan, G., Noor, Y.M., Liu, B., Ambikairaja, E., Webb, D.J., Peng, G.D.: A fast response intrinsic humidity sensor based on an etched singlemode polymer fiber Bragg grating. Sens. Actuators A Phys. **203**, 107–111 (2013)
13. Zhong, N., Liao, Q., Zhu, X., Zhao, M., Huang, Y., Chen, R.: Temperature-independent polymer optical fiber evanescent wave sensor. Sci. Rep. **5**, 1–10 (2015)
14. Leal-Junior, A., Frizera, A., Marques, C., José Pontes, M.: Polymer-optical-fiber-based sensor system for simultaneous measurement of angle and temperature. Appl. Opt. **57**(7), 1717 (2018)
15. Diaz, C.A.R., et al.: Liquid level measurement based on FBG-embedded diaphragms with temperature compensation. IEEE Sens. J. **18**(1), 193–200 (2018)
16. Ishikawa, R., et al.: Pressure dependence of fiber Bragg grating inscribed in perfluorinated polymer fiber. IEEE Photonics Technol. Lett. **29**(24), 2167–2170 (2017)
17. Peters, K.: Polymer optical fiber sensors—a review. Smart Mater. Struct. **20**(1), 13002 (2010)
18. Leal-Junior, A.G., Marques, C., Frizera, A., Pontes, M.J.: Dynamic mechanical analysis on a polymethyl methacrylate (PMMA) polymer optical fiber. IEEE Sens. J. **18**(6), 2353–2361 (2018)

19. Leal-Junior, A., Frizera-Neto, A., Marques, C., Pontes, M.: Measurement of temperature and relative humidity with polymer optical fiber sensors based on the induced stress-optic effect. Sensors **18**(3), 916 (2018)
20. Liu, Y., Peng, W., Liang, Y., Zhang, X., Zhou, X., Pan, L.: Fiber-optic Mach-Zehnder interferometric sensor for high-sensitivity high temperature measurement. Opt. Commun. **300**, 194–198 (2013)
21. Mizuno, Y., Hayashi, N., Fukuda, H., Song, K.Y., Nakamura, K.: Ultrahigh-speed distributed Brillouin reflectometry. Light Sci. Appl. **5**(12), e16184 (2016)
22. Perrotton, C., Javahiraly, N., Slaman, M., Dam, B., Meyrueis, P.: Fiber optic surface plasmon resonance sensor based on wavelength modulation for hydrogen sensing. Opt. Express **19**(S6), A1175 (2011)
23. Luo, Y., Yan, B., Zhang, Q., Peng, G.-D., Wen, J., Zhang, J.: Fabrication of polymer optical fibre (POF) gratings. Sensors **17**(3), 511 (2017)
24. Theodosiou, A., Lacraz, A., Stassis, A., Koutsides, C., Komodromos, M., Kalli, K.: Plane-by-plane femtosecond laser inscription method for single-peak bragg gratings in multimode CYTOP polymer optical fiber. J. Light. Technol. **35**(24), 5404–5410 (2017)
25. Cusano, A., Cutolo, A., Albert, J.: Fiber Bragg Grating Sensors: Market Overview and New Perspectives. Bentham Science Publishers, Potomac (2009)
26. Ashby, M.F.: Materials Selection in Mechanical Design. Elsevier, Cambridge (2005)
27. Abboud, R.J.: (i) relevant foot biomechanics. Orthopaedics **16**, 165–179 (2002)
28. Kirtley, C.: Clinical Gait Analysis: Theory and Practice. Elsevier, Philadelphia (2006)
29. Liu, Y., Lu, K., Yan, S., Sun, M., Lester, D.K., Zhang, K.: Gait phase varies over velocities. Gait Posture **39**(2), 756–760 (2014)
30. Shu, L., Hua, T., Wang, Y., Li, Q., Feng, D.D., Tao, X.: In-shoe plantar pressure measurement and analysis system based on fabric pressure sensing array. IEEE Trans. Inf. Technol. Biomed. **14**(3), 767–775 (2010)
31. Vilarinho, D., et al.: POFBG-embedded cork insole for plantar pressure monitoring. Sensors **17**(12), 2924 (2017)
32. Vilarinho, D., et al.: Foot plantar pressure monitoring with CYTOP Bragg Gratings sensing system. In: Proceedings of the 11th International Joint Conference on Biomedical Engineering Systems and Technologies, vol. 1, no. Biostec, pp. 25–29 (2018)
33. Thorlabs, Graded-Index Polymer Optical Fiber (GI-POF). https://www.thorlabs.com/catalogPages/1100.pdf. Accessed 17 May 2018
34. Antunes, P., Domingues, F., Granada, M., André, P.: Mechanical properties of optical fibers, pp. 1–15. INTECH Open Access Publisher (2012)
35. Suresh, R., Bhalla, S., Hao, J., Singh, C.: Development of a high resolution plantar pressure monitoring pad based on fiber Bragg grating (FBG) sensors. Technol. Health Care **23**, 785–794 (2015)
36. Domingues, M.F., et al.: Insole optical fiber sensor architecture for remote gait analysis - an eHealth solution. IEEE Internet Things J. **6**, 207–214 (2017)